
FROM EQUATIONS TO INSIGHTS: UNRAVELING SYMBOLIC STRUCTURES IN PDES WITH LLMs

Rohan Bhatnagar *

Department of Computer Science
University of Maryland, College Park
MD, 20742
rbhatna1@terpmail.umd.edu

Ling Liang

Department of Mathematics
University of Maryland, College Park
MD, 20742
liang.ling@u.nus.edu

Krish Patel

Department of Computer Science
University of Maryland, College Park
MD, 20742
kripatel@terpmail.umd.edu

Haizhao Yang

Department of Mathematics
Department of Computer Science
University of Maryland, College Park
MD, 20742
hzyang@umd.edu

ABSTRACT

Motivated by the remarkable success of artificial intelligence (AI) across diverse fields, the application of AI to solve scientific problems—often formulated as partial differential equations (PDEs)—has garnered increasing attention. While most existing research concentrates on theoretical properties (such as well-posedness, regularity, and continuity) of the solutions, alongside direct AI-driven methods for solving PDEs, the challenge of uncovering symbolic relationships within these equations remains largely unexplored. In this paper, we propose leveraging large language models (LLMs) to learn such symbolic relationships. Our results demonstrate that LLMs can effectively predict the operators involved in PDE solutions by utilizing the symbolic information in the PDEs. Furthermore, we show that discovering these symbolic relationships can substantially improve both the efficiency and accuracy of the finite expression method for finding analytical approximation of PDE solutions, delivering a fully interpretable solution pipeline. This work opens new avenues for understanding the symbolic structure of scientific problems and advancing their solution processes.

Keywords Large Language Models · Finite Expression Method · High Dimensional PDEs · Operator Relation

1 Introduction

Numerous grand challenges in scientific fields, including physics, engineering, biology, and chemistry, can be modeled as partial differential equations (PDEs), which relate unknown functions defined on a multidimensional domain (e.g., in terms of space and time) to its rates of change with respect to each of those variables [Evans, 2022]. Mathematically, a PDE takes the following form

$$Du(x) = f(u(x), x), \quad x \in \Omega, \quad Bu(x) = g(x), \quad x \in \partial\Omega, \quad (1)$$

where D denotes a certain differential operator defining the dynamics, $Bu = g$ represents the boundary condition (such as Dirichlet, Neumann, and Robin), and $\Omega \subseteq \mathbb{R}^d$ describes the domain with boundary $\partial\Omega$.

PDEs often arise in high-dimensional settings (i.e., d is large); for example, well-known instances such as the Poisson equation [Yu et al., 2018], the linear conservation law [Chen et al., 2021], and the nonlinear Schrödinger equation [Han et al., 2020] regularly involve multiple spatial and temporal variables. While low-dimensional PDEs can be solved

*The first three authors contribute equally.

reliably and efficiently via traditional mesh-dependent methods such as finite difference methods [LeVeque, 2007], finite elements methods [Hughes, 2003], finite volume methods [Toro, 2013], and spectral methods [Boyd, 2001], developing efficient and accurate algorithmic frameworks for computing numerical solutions to high-dimensional PDEs remains an important and challenging topic due to the curse of dimensionality (i.e., the computational costs grow exponentially with respect to the dimensionality of the problem’s domain) [E et al., 2021].

Before solving a PDE, one must understand certain fundamental properties of the solution $u(x)$ that follow from the PDE itself and from the data—namely, $f(u(x), x)$ and $g(x)$. These considerations align with the classical theory of PDEs [Evans, 2022], which focuses on establishing well-posedness (i.e., the existence and uniqueness of solutions) and their regularity and continuity. However, the underlying symbolic relationship among u , f and g often remains underexplored. To address this gap, we pose the following question:

Assuming that the PDE (1) admits an analytical solution u , and given the operators appearing in the expressions of f and g , what are the corresponding operators in the expression for u ?

Understanding this symbolic connection is crucial for deriving fully interpretable, closed-form solutions, a feature lacking in most existing solution methods, particularly in the high-dimensional setting. As an illustrative example, we consider solving the PDE (1) via the least square method [Dissanayake and Phan-Thien, 1994, Lagaris et al., 1998, Sirignano and Spiliopoulos, 2018], which defines a straightforward functional to characterize the error of the estimated solution by

$$L(u) = \|Du - f\|_{L^2(\Omega)}^2 + \lambda \|Bu - g\|_{L^2(\partial\Omega)}^2, \quad (2)$$

where $\lambda > 0$ balances the influence of boundary conditions. The goal is to find a function $u^* \in L^2(\Omega)$ so that the least square loss is minimized, i.e.,

$$u^* = \operatorname{argmin}_{u \in L^2(\Omega)} L(u). \quad (3)$$

Because the search space $L^2(\Omega)$ is an infinite dimensional space, finding the solution u^* is extremely challenging. Fortunately, the search space can be significantly simplified if one knows the operators appearing in the solution in advance, making the search of the optimal solution much easier and effective. This can be accomplished by adopting the recently developed finite expression method (FEX) [Liang and Yang, 2022].

To uncover the symbolic relationship described above, we leverage large language models (LLMs) as predictive tools. The process begins with the generation of a comprehensive, structured dataset composed of symbolic expressions derived from a diverse range of PDE types, including elliptic, parabolic, and hyperbolic equations, along with their associated boundary and initial conditions. These symbolic expressions are represented as computational trees (see Figure 1), where nodes are populated with unary (e.g., \sin , \cos , \exp) and binary operators (e.g., $+$, $-$, $*$, $/$). This tree structure captures the hierarchical nature of mathematical expressions and ensures a systematic representation of the PDE solutions.

To prepare the data for LLM processing, the symbolic expressions are tokenized and converted into postfix notation (Reverse Polish Notation). This format is chosen because it aligns well with the sequential input requirements of LLMs and eliminates the need for parentheses, simplifying the parsing process. More importantly, it reflects the relative positional relationship of operators in the expression. The tokenized dataset is then used to fine-tune foundational LLMs such as T5, BART, and Llama. During fine-tuning, the models are trained to predict the sequence of operators that constitute the symbolic solution to a new PDE. The training objective is to maximize the accuracy of operator sequence prediction, ensuring that the model can reliably identify the minimal set of operators required to represent the true solution.

Once fine-tuned, the LLM acts as a predictive tool to generate operator sets for new PDE problems. The predicted operator sets are highly refined, containing only the operators necessary to construct the solution, thereby eliminating redundant or irrelevant operators. This refinement is crucial for the subsequent application of the finite-expression method (FEX), a reinforcement learning based symbolic regression technique that searches for the optimal combination of operators and constants to approximate the PDE solution. By providing FEX with a reduced and targeted operator set, the combinatorial search space is significantly narrowed. This reduction not only enhances the accuracy of the solution by focusing on relevant operators, but also dramatically improves computational efficiency by reducing the number of potential combinations that need to be evaluated.

In summary, the integration of LLMs into this workflow transforms the process of symbolic PDE solving. By generating structured datasets, fine-tuning models to predict operator sequences, and leveraging these predictions to guide FEX, we achieve a more accurate and computationally efficient approach to discovering symbolic solutions for complex PDEs. This methodology bridges the gap between machine learning and symbolic mathematics, offering great potential for scientific computing and engineering applications. Particularly, our contributions are summarized as follows:

(1) We formally pose the problem of discovering the symbolic relationship between the solution of a PDE and the associated problem data, including the boundary conditions and right-hand-side functions. Establishing this connection can provide deeper insights into the underlying structure of PDEs, enabling more precise analytical solutions and facilitating the development of efficient numerical methods which provides high-quality analytical solutions. By highlighting the potential impact of such relationships, our work lays the foundation for further studies in this area, aiming to bridge the gap between problem formulation and solution representation.

(2) We propose fine-tuning LLMs to learn the symbolic relationship between problem data and the solution of a PDE, demonstrating remarkable effectiveness in predicting the operators that characterize the solution. By integrating this approach with the FEX method, our numerical findings show that while LLMs may not be inherently suited for directly solving PDEs or other complex scientific problems, they provide substantial benefit in identifying underlying structures and symbolic patterns. This capability significantly streamlines and enhances the solution process. Our work underscores the potential of LLMs as transformative tools in the analytical and computational study of PDEs, bridging the gap between symbolic reasoning and sophisticated mathematical problem-solving.

1.1 Related work

Artificial intelligence (AI) for Science takes advantage of modern advanced machine learning (ML) methods to facilitate, accelerate and enhance scientific discovery [Stevens et al., 2020]. Its importance lies in the ability to handle massive datasets, uncover hidden patterns, and simulate complex phenomena. Inspired by the remarkable success of AI across various domains, deep neural network (DNN)-based approaches [LeCun et al., 2015, Goodfellow, 2016] have become increasingly popular for solving (high-dimensional) PDEs. These methods offer certain appealing advantages over traditional numerical techniques, making them a compelling alternative for tackling complex problems. First, DNN-based approaches empirically mitigate the curse of dimensionality that plagues conventional discretization approaches, leading to more efficiency in handling high-dimensional PDEs Han et al. [2018]. Second, DNNs, acting as mesh-free universal function approximators [Cybenko, 1989, Hornik et al., 1989, Goodfellow, 2016], can be trained to learn highly complex PDE solutions without the need of prespecifying basis functions or meshes [Berg and Nyström, 2018, Raissi et al., 2019]. Hence, they are highly suitable to approximate complex solution spaces that challenges the traditional mesh-based approaches. Third, the solutions represented by DNNs can be evaluated efficiently once trained, which turns out to be a crucial property for tasks, including uncertainty quantification and real-time optimal control, require calling PDE solutions repeatedly [Zhu et al., 2019]. Last but not least, continuous progress in designing comprehensive neural network architectures—such as Fourier neural operators and advanced physics-informed neural network frameworks—alongside theoretical advancements in understanding their approximation capabilities, are making these methods increasingly applicable [Lu et al., 2019, Li et al., 2020].

However, several critical factors often hinder deep neural networks (DNNs) from achieving highly accurate solutions, even for relatively simple problems. These include the need for large, diverse, and high-quality training data [Szegedy, 2013, Buda et al., 2018], sensitivity to hyperparameter selection [Bergstra and Bengio, 2012], the challenge of optimizing highly nonconvex objectives [Dauphin et al., 2014, Choromanska et al., 2015], issues like vanishing and exploding gradients [Glorot and Bengio, 2010], and poor generalization capabilities [Zhang et al., 2021]. Additionally, solutions produced by DNNs often lack interpretability, preventing users from leveraging insights for future decision-making [Rudin, 2019]. To overcome these challenges and achieve both highly accurate and interpretable solutions for PDEs, Liang and Yang [2022] recently introduced the finite expression method (FEX). This approach leverages recent advances in approximation theory, which demonstrate that high-dimensional functions can be effectively approximated using functions composed of simple operators [Shen et al., 2021a,b, Zhang et al., 2022]. This methodology seeks approximate PDE solutions within the space of functions composed of finitely many analytic expressions, effectively avoiding the curse of dimensionality. In FEX, the mathematical expression representing the PDE solution is modeled as a binary tree, where each node holds either a unary or binary operator chosen from pre-specified operator sets. The goal is to find the optimal sequence of operators and coupling parameters that minimize the objective function associated with the PDE. This leads to a combinatorial optimization (CO) problem, which is then solved by a deep reinforcement learning (RL) method with the policy gradient optimizer. The FEX outperforms certain existing numerical PDE solvers in terms of accuracy, interpretability and memory efficiency, making it a promising approach for solving high-dimensional PDEs and other complex problems; see e.g., [Song et al., 2023, 2024, Hardwick et al., 2024].

2 Methodology

In this section, we propose a novel method that fine-tunes large language models (LLMs) to predict the operator sets present in the symbolic expressions of partial differential equation (PDE) solutions. Our approach consists of three main

stages: data generation, model fine-tuning, and performance evaluation. Below, we detail the pipeline for generating synthetic data, the procedure for fine-tuning the LLMs, and the evaluation of their predictive capabilities.

2.1 Binary Computational Trees for PDE Expressions

Expressions in PDEs are represented as **binary computational trees**, as depicted in Figure 1. These trees provide a structured and hierarchical way to encode mathematical expressions, enabling efficient exploration and manipulation of the solution space. The tree generation process is systematic and begins by specifying the **depth** of the binary tree, which determines the complexity and granularity of the resulting expressions.

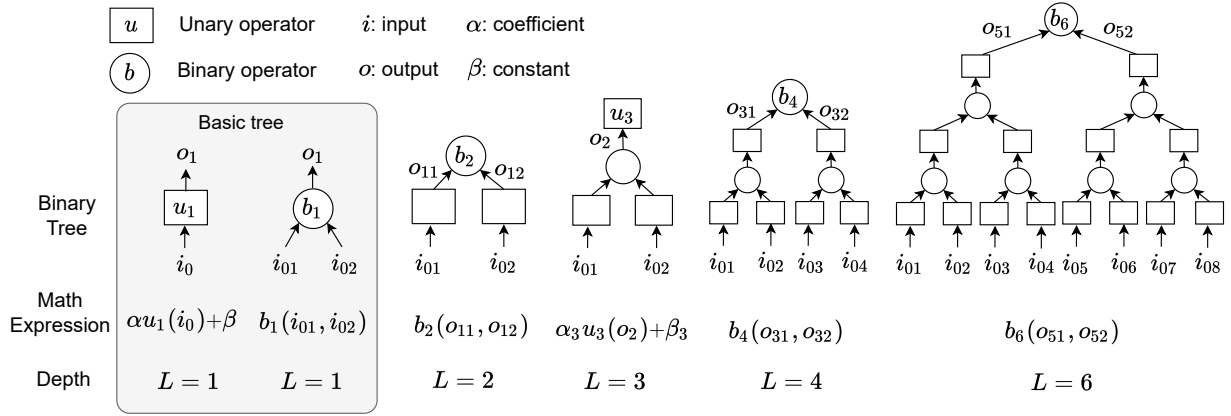


Figure 1: Computational expression tree [Liang and Yang, 2022].

The construction of the tree involves the following steps:

1. **Depth Specification:** The depth of the tree is predefined, controlling the number of hierarchical levels in the tree. A deeper tree allows for more complex expressions but increases computational cost.
2. **Recursive Construction:** At each level of depth, the tree is built recursively. Starting from the root node, each node is expanded by adding child nodes according to the rules defined for operators. This recursive process ensures a systematic exploration of the solution space, covering a wide range of possible expressions.

Each node in the computational tree represents an operator, which can be either a **unary operator** or a **binary operator**:

- **Unary Operators:** These operators act on a single operand and include functions such as trigonometric functions ($\sin(\cdot)$, $\cos(\cdot)$, $\tan(\cdot)$), exponential functions ($\exp(\cdot)$), logarithmic functions ($\lg(\cdot)$, $\ln(\cdot)$), and other nonlinear transformations ($\sqrt{\cdot}$, $|\cdot|$, $(\cdot)^k$, $k \in \mathbb{Z}$). For each node with a unary operator, *two scalars* (α and β) are coupled with the node. These scalars enable the composition of the underlying operation with an *affine function*, resulting in expressions of the form $\alpha \cdot u(\cdot) + \beta$, where $u(\cdot)$ is the unary operation. This coupling ensures that the tree can represent both nonlinear transformations and linear adjustments, enhancing its expressive power.
- **Binary Operators:** These operators require two operands and include standard arithmetic operations including addition (+), subtraction (-), multiplication (\times) and division (/). Binary operators combine two sub-expressions (left and right child nodes) to form more complex expressions. For example, a multiplication node might combine the results of two subtrees representing different terms in an expression.

The use of binary computational trees offers several advantages: (1) The tree structure provides a clear and interpretable representation of mathematical expressions, making it easier to analyze and manipulate them; (2) By recursively constructing trees of varying depths, the method ensures a thorough exploration of the solution space, capturing both simple and complex expressions; and (3) The inclusion of both unary and binary operators, along with affine transformations, allows the tree to represent a wide range of mathematical operations and relationships. By systematically generating and evaluating computational trees, it becomes possible to identify candidate expressions that best describe the underlying dynamics of a system. Additionally, the framework can be combined with advanced techniques, including optimization and reinforcement learning, to refine the scalars and operators, further improving the accuracy of the discovered models.

2.2 Data Generation for Equation Types

In this subsection, we describe the data generation process for constructing a structured dataset of symbolic expressions derived from various PDE types. The dataset is designed to capture the symbolic relationships between the solution of a PDE and the associated problem data, including the boundary conditions and right-hand-side functions. The data generation process is outlined in Figure 2.

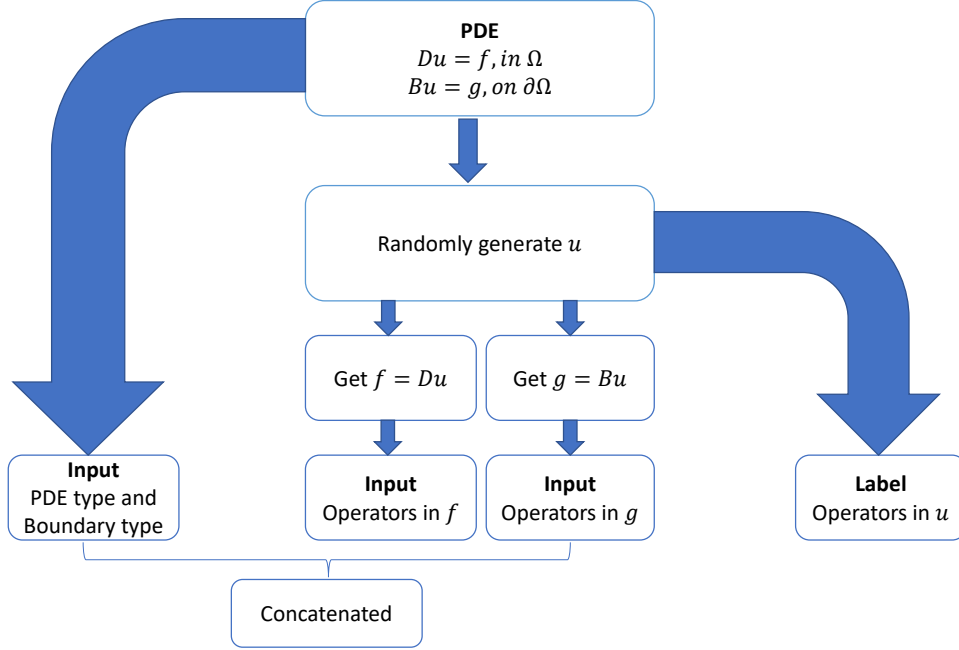


Figure 2: Data generation pipeline.

The construction of the one data point involves the following steps.

PDE Type Specification. We first specify the type of PDE (e.g., Poisson, linear conservation law, and Schrödinger) and the type of boundary conditions (e.g., Dirichlet, Neumann and Robin) based on the information of the operators D and B . This results in the first component of the data point, which includes the PDE type and boundary condition type of the data point.

Randomly generated function $u(x)$. Next, we generate a random function $u(x)$ by constructing a binary computational tree with a specified depth, as described in Section 2.1. The tree is populated with random unary and binary operators drawn from prescribed operator sets that are rich enough. Consequently, we obtain the expression tree for the solution function $u(x)$, which is used to derive the second component of the data point, i.e., expressions of the right-hand-side function f and the function g defined on the boundary of the domain.

Postfix Representation. After obtaining the expressions of the functions $u(x)$, $f(u(x), x)$, and $g(x)$, we convert them into postfix notation. This conversion simplifies the tokenization process and aligns the expressions with the input format required by LLMs. The postfix notation also eliminates the need for parentheses, making the expressions more interpretable and easier to parse. More importantly, it reflects the relative positional relationship of operators in the expression, which is crucial for the LLMs to learn the symbolic relationships between the operators. In the end, we obtain the second component of the data point, which includes the operators used in the right-hand-side function $f(u(x), x)$, and the function $g(x)$. These input component are then concatenated to generate the input. Meanwhile, the label of the data set is obtained similarly by converting the expression of the function $u(x)$ into postfix notation. See Figure 3 for the detailed conversion pipeline and a simple illustrated example.

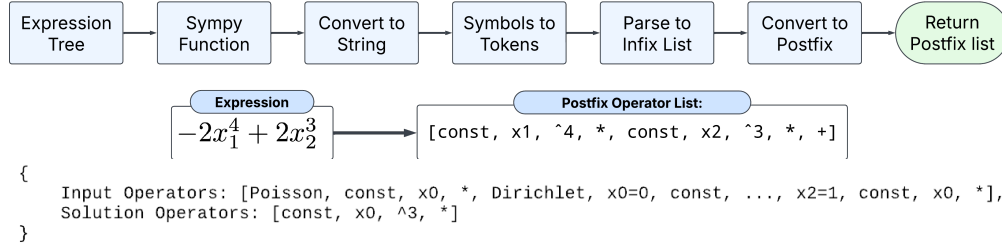


Figure 3: Pipeline for converting data into postfix notation and an illustrated example.

2.3 Fine-tuning

Inspired by the success of LLMs, we propose fine-tuning the *sequence-to-sequence* Transformer architecture that leverages cross-attention to incorporate PDE context when generating solution operators. This architecture is selected because it effectively captures long-range dependencies and the complex hierarchical structure inherent in PDE metadata, thereby learning an effective mapping between symbolic operator sequences.

We first preprocess and tokenize the dataset generated as in the previous subsection, and then fine-tune the LLM using the proceed data using the common practices in the literature. The whole pipeline is outlined in Figure 4 and the key components in the pipeline are discussed in detailed as follows.

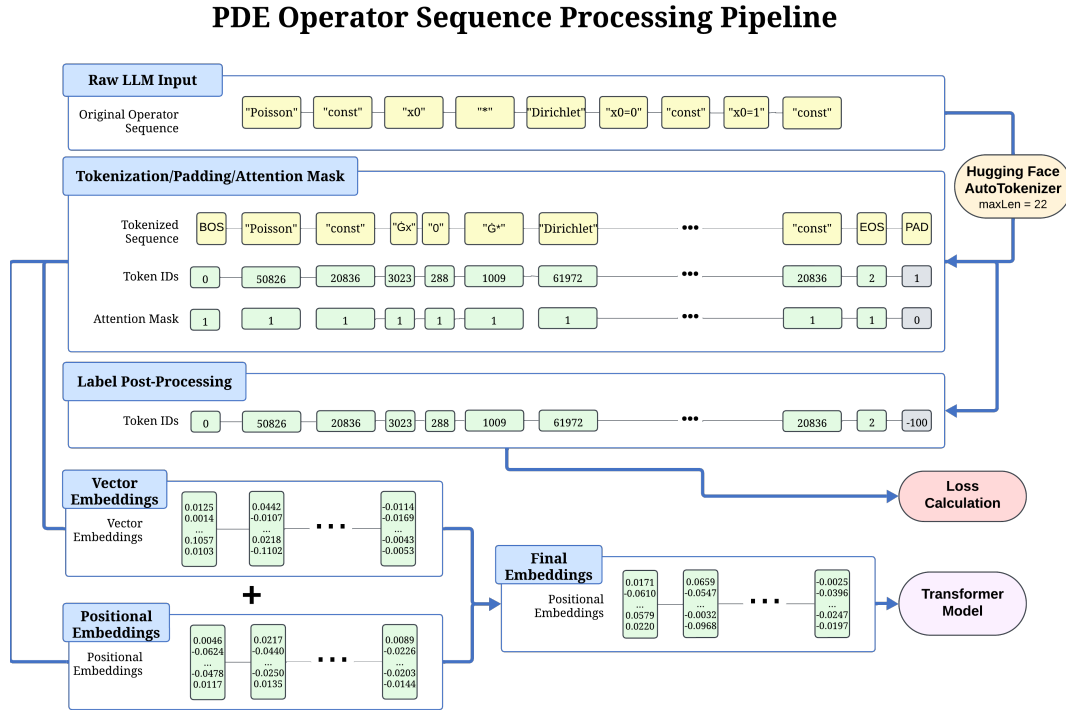


Figure 4: Pipeline for tokenization and embedding of operator sequences for LLM fine-tuning

Tokenization. We begin by loading the PDE data in jsonl format, shuffling it, and splitting it into training and validation sets. Each data point is then processed by a textual embedding layer that converts operator symbols (e.g., *sin*, *cos*, *exp*) into tokens. To ensure a robust and consistent representation, we use HuggingFace’s ² AutoTokenizer, which selects an appropriate tokenization scheme based on the underlying pre-trained model. The tokenizer pads sequences to a fixed length and incorporates learnable positional embeddings. Additionally, an attention mask is generated to differentiate between valid and padding tokens, facilitating self-attention computations. Finally, padding tokens

²<https://github.com/huggingface>

in the label sequences are replaced with -100 , the default `ignore_index` in PyTorch’s `nn.CrossEntropyLoss`, ensuring they are ignored during loss computation. This approach standardizes the transformation of textual operator representations into numerical tokens for model training.

Architecture and Finetuning: Next, we select a pretrained LLM with a sequence-to-sequence Transformer architecture. We fine-tune this model using the HuggingFace `Trainer` API, which provides a suite of tools for efficient optimization. During fine-tuning, we minimize the token-wise cross-entropy loss, which penalizes incorrect token predictions, including misclassification of the End-of-Sequence (EOS) token. Backpropagation is performed to update the model’s parameters according to the optimization algorithm. We emphasize the use of teacher forcing⁴ during fine-tuning. By supplying the decoder with the full target sequence, this approach ensures that the token-wise cross-entropy loss is computed over aligned positions, preventing error accumulation and reinforcing the correct sequential dependencies more effectively and robustly.

2.4 Inferencing

Once trained, the model can predict operator sets in solutions for *new* PDEs. Specifically, we provide the language model with a data point consisting of the PDE type, its right-hand side (RHS), and the associated boundary condition, as described in Section 2.2. This data is then tokenized following the procedure outlined in the previous subsection. The language model’s decoder then auto-regressively generates an operator sequence representing the solution, with each predicted token conditioned on previously decoded tokens and the input context. While the exact sequential order may vary slightly, the model consistently identifies the correct set of operators, prioritizing presence over strict ordering.

Since the model’s output is a numerical vector, a final post-processing step is required to extract the predicted operators. First, we extract the unique operators by removing duplicates from the predicted postfix representation, ensuring that only essential components remain. Because the model is trained to reproduce entire operator sequences rather than direct sets, this step distills the output into a concise and meaningful form. Next, the obtained set is checked for misspellings and tokenization errors. Given that the model generates sequences based on learned patterns rather than strict syntax rules, occasional character-level errors may arise, particularly with uncommon symbols or operators. To ensure correctness and consistency, any malformed operators are discarded.

To evaluate the accuracy of the fine-tuned LLM, we use the squared norm to quantify the discrepancy between the predicted operator set and the ground-truth label. Particularly, given a dictionary of all possible operators of size n , each operator set is represented as a binary vector, as illustrated in Table 1.

Function	Preprocessed Operator Set	Binary Vector								
		x_1	x_2	\wedge^2	\wedge^3	+	*	SIN	COS	EXP
$(5x_1)^2 + \sin(3x_2) \cdot x_2$	[x_1 , x_2 , \wedge^2 , +, *, SIN]	1	1	1	0	1	1	1	0	0
$5 \exp(2x_1) \cdot (\cos(6x_1))^3$	[x_1 , \wedge^3 , *, COS, EXP]	1	0	0	1	0	1	0	1	1

Table 1: Sample binary-vector encoding for two example expressions. The size of the dictionary is 9.

Then, the squared distance between two such operator sets, represented by vectors $y \in \mathbb{R}^n$ and $z \in \mathbb{R}^n$, can be defined as

$$\|y - z\|^2 = \sum_{i=1}^n (y_i - z_i)^2.$$

Clearly, it measures the number of mismatched operators between the two operator sets. Moreover, this metric prioritizes the presence of operators over their sequence order, ensuring that the predicted operators remain useful for numerical and analytical PDE solving, as well as for scientific analysis of PDE models.

3 Experimental Results

In this section, we conduct extensive experiments to evaluate the effectiveness of our proposed approach. Our evaluation consists of two main components: (1) assessing the predictive performance of fine-tuned large language models (LLMs)

³<https://pytorch.org/>

⁴Teacher forcing is a training strategy where, at each time step, the decoder is provided with the actual ground-truth token instead of its own previous prediction.

in identifying operator sets within PDE solutions and (2) demonstrating the practical impact of these predictions in guiding operator selection within the finite expression method (FEX).

First, we analyze the ability of fine-tuned LLMs to predict the correct operator sets in PDE solutions. The objective is to assess whether the models can effectively learn and generalize the symbolic relationships between PDE solutions and problem data. We compare the predicted operator sets against ground-truth labels to measure the accuracy of the learned representations. Additionally, we examine the impact of model architecture by fine-tuning several commonly used open-source LLMs.

Second, we apply the fine-tuned LLMs to enhance the efficiency and accuracy of the FEX method by leveraging their predicted operator sets. This experiment attempts to achieve two goals. On one hand, we demonstrate that by obtaining more precise operator sets of smaller sizes, the computational costs spent in FEX can be significantly reduced. On the other hand, we evaluate whether FEX achieves improved accuracy in learning PDE solutions when provided with the correct prior information about the relevant operators. By comparing FEX solutions obtained with and without LLM-guided operator selection, we quantify improvements in both computational efficiency and numerical accuracy.

Through these experiments, we aim to establish the viability of fine-tuned LLMs as effective tools for discovering symbolic relations in PDE solutions and enhancing PDE-solving techniques.

3.1 Experimental Setup

For data generation, we consider two types of PDEs—namely, the Poisson equation and the linear conservation law—each paired with three commonly used boundary conditions: Cauchy, Dirichlet, and Neumann. Using a tree depth of 3, we randomly generate a dataset of 60,000 equations, with 30,000 examples for each PDE type, as described in Section 2.2. This dataset is then used to fine-tune two state-of-the-art large language models: BART [Lewis et al., 2019] and T5 [Raffel et al., 2020].

For fine-tuning, we optimize the cross-entropy loss using the AdamW optimizer with a learning rate of 2×10^{-5} and a weight decay of 0.01. The models are trained for 3 epochs with a batch size of 2. Fine-tuning is conducted on an NVIDIA A6000 GPU with 48 GB of memory. To efficiently manage storage, we save checkpoints every 500 steps and retain only the three most recent checkpoints.

Finally, we integrate the model into the FEX solver⁵. During the execution of FEX for a given PDE, the model is invoked for inference. After inference, the post-processing step detailed in Section 2.4 is applied to extract the unique unary and binary operator sets. These sets are then used to configure the available operators within FEX during its search for an analytical PDE solution. We refer to this version of FEX as the "LLM-informed FEX" and denote the original FEX as "uninformed FEX." The uninformed FEX employs a fixed operator set:

$$\text{Binary set: } \mathbb{B} = \{+, -, *\}, \quad \text{Unary set: } \mathbb{U} = \{0, 1, \text{Id}, (\cdot)^2, (\cdot)^3, (\cdot)^4, \exp, \sin, \cos\}.$$

In contrast, the LLM-informed FEX dynamically predicts the operator sets for each example, enabling a more adaptive and potentially efficient search process.

3.2 Effectiveness of Fine-tuned LLMs

In this subsection, we evaluate the performance of the fine-tuned BART and T5 models in predicting operator sets for the two PDE types. Specifically, we track the training and validation losses throughout the training process, as well as the average number of mismatched operators on the test dataset for each epoch. The computational results are summarized in Tables 2 and 3.

Epoch	Training Loss	Validation Loss	Average Mismatch
1	0.058200	0.057948	2.475833
2	0.040000	0.046193	2.020000
3	0.039200	0.038100	1.720210

Table 2: Fine-tuning BART on large dataset.

⁵For a detailed description of the FEX method, we refer the reader to Liang and Yang [2022], and for the implementation of the original FEX, see <https://github.com/LeungSamWai/Finite-expression-method>.

Epoch	Training Loss	Validation Loss	Average Mismatch
1	0.046800	0.045303	1.711056
2	0.037200	0.036140	1.544056
3	0.012300	0.020392	1.012000

Table 3: Fine-tuning T5 on large dataset.

Both fine-tuned models exhibit a consistent decrease in training and validation loss across epochs, indicating successful fine-tuning. However, T5 demonstrates a more pronounced reduction in both loss metrics. The larger gap between BART’s training and validation loss suggests that it may be more prone to overfitting compared to T5, which appears to generalize better. In terms of the average number of mismatched operators, T5 consistently outperforms BART in this regard across all epochs. The sharper decline in mismatch for T5 suggests that it adapts more effectively to the symbolic representation of PDE solutions and captures the underlying operator structures with higher precision. Overall, T5 demonstrates superior performance in predicting operators for PDE solutions, making it a more suitable choice for integration into the LLM-informed FEX solver. In light of these findings, we incorporate the fine-tuned T5 model into the FEX framework to enhance its operator selection process.

3.3 LLM-informed FEX

In this subsection, we evaluate the effectiveness of the LLM-informed FEX using the fine-tuned T5 model in comparison to the uninformed FEX. As an initial validation step, we conduct a sanity check using several simple examples to ensure the correctness of the approach. To comprehensively assess the performance of the proposed framework, we further test both versions of FEX on a dataset of 100 randomly generated PDEs, consisting of 50 Poisson equations and 50 linear conservation law equations.

3.3.1 Sanity Check

We first construct 4 Poisson equations and 4 linear conservation law equations, whose true solutions, denoted as $u(x)$, are randomly handcrafted. For each example, we present the Binary and Unary set sizes, the number of iterations and computational time taken to find the approximate solution, and the error with respect to the true solution. The results are summarized in Tables 4 and 5, respectively.

$u(x)$	Method	Binary Size	Unary Size	Iters	Time [m]	Error
$4 \cos(4x^2 \cos(x_0))$	LLM-informed	1	2	4.25	8.25	0
	Uninformed	3	9	167	340	0
$4x_1^3 + 4x_1^2 + 2 \cos(4x_1^3 \cos(x_0))$	LLM-informed	2	4	102	286	10^{-8}
	Uninformed⁶	3	9	2000+	2400+	N/A
$128x_2^3 + 2x_2e^{4x_2^4}$	LLM-informed	2	4	34.5	40.5	4×10^{-7}
	Uninformed	3	9	90	186	6×10^{-7}
$64x_1^2e^{2x_2}$	LLM-informed	1	3	15.5	21	3×10^{-8}
	Uninformed	3	9	103.5	161	3×10^{-8}

Table 4: Sanity check for the Poisson equation.

⁶Uninformed FEX did not converge within 2000 iterations, indicated by “2000+” (iterations) and “N/A” for error.

$u(x)$	Method	Binary Size	Unary Size	Iters	Time [m]	Error
$\sin\left(x_1 + \frac{\pi}{4}x_2 + \frac{\pi}{4}x_3\right)$	LLM-informed	2	2	1	0.3	0
	Uninformed	3	9	3	1	0
$4(2x_0 - 2x_2^3)^3$	LLM-informed	2	2	2	0.6	0
	Uninformed	3	9	33.3	9.4	0
$8x_2^2 + 8\sin(x_1)$	LLM-informed	2	3	1	1	0
	Uninformed	3	9	24	28.5	0
$16\sin^3(x_0) + 2\sin(2x_1 + 2\sin(x_2))$	LLM-informed	2	3	39	100	0
	Uninformed	3	9	273	488	0

Table 5: Sanity check for the linear conservation law equation.

The computational results presented in Tables 4 and 5 demonstrate that the LLM-informed FEX significantly improves efficiency over the uninformed FEX while maintaining high accuracy. One major advantage is the reduction in the number of required operators. The uninformed FEX consistently uses a fixed operator set of 3 binary and 9 unary operators, whereas the LLM-informed FEX dynamically selects a smaller, more relevant subset—typically with at most 2 binary and 4 unary operators. This reduced search space leads to a dramatic decrease in the number of iterations required for convergence. For instance, in the first Poisson equation example, the LLM-informed FEX requires only 4.25 iterations compared to 167 for the uninformed version, and in another case, the uninformed FEX exceeds 2000 iterations without converging, while the LLM-informed approach successfully completes the solution in 102 iterations. This efficiency gain translates into significant computational time savings, with the LLM-informed approach solving problems up to an order of magnitude faster. Despite this drastic reduction in computational cost, the accuracy remains comparable; for cases where the uninformed FEX converges, both methods yield similar approximation errors, and for the linear conservation law equations, both achieve exact solutions. These results highlight the effectiveness of integrating the fine-tuned T5 model into the FEX framework, demonstrating that LLM-informed operator selection leads to a more efficient and reliable symbolic PDE solver.

3.3.2 Randomly Generated PDEs

To further validate the reliability of our approach, we evaluated the performance of the FEX algorithm on a set of randomly generated PDE examples.

For each PDE type, we randomly generated 50 instances using a depth-2 computational tree structure, as described in Section 2.2. Since FEX is a randomized reinforcement learning approach, each instance was solved five times to obtain average computational results, including the number of iterations until convergence, computation time, and solution error. The FEX algorithm was limited to a maximum of 150 iterations and an error tolerance of 10^{-3} (i.e., $\varepsilon < 1 \times 10^{-3}$), where ε was computed during training using a composite loss that combines PDE residuals and boundary violations over a set of sampled points from the domain and its boundary, respectively. A PDE instance was considered successfully solved if the desired accuracy was achieved within 150 iterations. The computational results are summarized in Tables 6 and 7.

Table 6: Summary Statistics for Poisson PDEs

Metric	Uninformed FEX	LLM-Informed FEX	Improvement (Reduction)
Success Ratio (Valid Solutions)	51.06% (24/47)	68.09% (32/47)	↑ 33.35%
For Cases Where BOTH Versions Yield Valid Solutions			
Mean Iterations	61.80	27.87	↓ 54.90%
Mean Duration (min)	40.73	20.25	↓ 50.27%

Table 7: Summary Statistics for Linear Conservation Law PDEs

Metric	Uninformed FEX	LLM-Informed FEX	Improvement (Reduction)
Success Ratio (Valid Solutions)	66.67% (30/45)	64.44% (29/45)	↓ 3.46%
For Cases Where BOTH Versions Yield Valid Solutions			
Mean Iterations	24.87	13.98	↓ 43.80%
Mean Duration (min)	6.43	3.60	↓ 44.03%

The results in Tables 6 and 7 indicate that the LLM-informed FEX method consistently accelerates convergence compared to the Uninformed FEX, though its impact on solution validity varies across PDE types. For Poisson PDEs, the LLM-informed approach significantly improves the success ratio, increasing it by 33.35% (from 51.06% to 68.09%), while also reducing the number of iterations by 54.90% and computation time by 50.27%. This suggests that incorporating LLM-informed heuristics enhances both accuracy and efficiency for this class of problems. However, for linear conservation law PDEs, the LLM-informed approach slightly reduces the success ratio by 3.46%, indicating that its effectiveness in improving solution validity may be problem-dependent. This decline appears to stem from the inherent instability of FEX, even when accurate operators are provided. Despite this, the LLM-informed method still achieves a 43.80% reduction in iterations and a 44.03% decrease in computation time, demonstrating substantial gains in computational efficiency.

Overall, the LLM-informed approach consistently accelerates convergence, making it a valuable tool for solving PDEs more efficiently. However, its impact on solution validity remains inconsistent. This suggests that while the LLM-informed approach effectively reduce computational costs, one may need to conduct further refinement to the PDE solver itself to improve robustness across different PDE types.

4 Conclusions

In this work, we explored the potential of large language models (LLMs) to uncover symbolic relationships in partial differential equations (PDEs), a largely unexplored challenge in the intersection of AI and scientific computing. Our results demonstrate that fine-tuned LLMs can effectively predict the operators involved in PDE solutions by leveraging symbolic information from the governing equations. By integrating these predictions into the finite expression method (FEX), we significantly enhanced both the efficiency and accuracy of analytical PDE approximations. Compared to the traditional uninformed FEX, the LLM-informed approach reduces the number of operators required, accelerates convergence, and maintains high solution accuracy, providing a fully interpretable and computationally efficient pipeline. These findings highlight the promising role of LLMs in advancing symbolic reasoning for scientific problems, paving the way for further exploration of AI-driven methodologies in mathematical modeling and equation solving.

Acknowledgement

The authors were partially supported by the US National Science Foundation under awards DMS-2244988, DMS-2206333, the Office of Naval Research Award N00014-23-1-2007, and the DARPA D24AP00325-00.

References

- J. Berg and K. Nyström. A unified deep artificial neural network approach to partial differential equations in complex geometries. *Neurocomputing*, 317:28–41, 2018.
- J. Bergstra and Y. Bengio. Random search for hyper-parameter optimization. *Journal of machine learning research*, 13(2), 2012.
- J. P. Boyd. *Chebyshev and Fourier spectral methods*. Courier Corporation, 2001.
- M. Buda, A. Maki, and M. A. Mazurowski. A systematic study of the class imbalance problem in convolutional neural networks. *Neural networks*, 106:249–259, 2018.
- J. Chen, S. Jin, and L. Lyu. A deep learning based discontinuous Galerkin method for hyperbolic equations with discontinuous solutions and random uncertainties. *arXiv preprint arXiv:2107.01127*, 2021.
- A. Choromanska, M. Henaff, M. Mathieu, G. B. Arous, and Y. LeCun. The loss surfaces of multilayer networks. In *Artificial intelligence and statistics*, pages 192–204. PMLR, 2015.

- G. Cybenko. Approximation by superpositions of a sigmoidal function. *Mathematics of control, signals and systems*, 2(4):303–314, 1989.
- Y. N. Dauphin, R. Pascanu, C. Gulcehre, K. Cho, S. Ganguli, and Y. Bengio. Identifying and attacking the saddle point problem in high-dimensional non-convex optimization. *Advances in neural information processing systems*, 27, 2014.
- M. G. Dissanayake and N. Phan-Thien. Neural-network-based approximations for solving partial differential equations. *communications in Numerical Methods in Engineering*, 10(3):195–201, 1994.
- W. E, J. Han, and A. Jentzen. Algorithms for solving high dimensional PDEs: from nonlinear Monte Carlo to machine learning. *Nonlinearity*, 35(1):278, 2021.
- L. C. Evans. *Partial differential equations*, volume 19. American Mathematical Society, 2022.
- X. Glorot and Y. Bengio. Understanding the difficulty of training deep feedforward neural networks. In *Proceedings of the thirteenth international conference on artificial intelligence and statistics*, pages 249–256. JMLR Workshop and Conference Proceedings, 2010.
- I. Goodfellow. Deep learning, 2016.
- J. Han, A. Jentzen, and W. E. Solving high-dimensional partial differential equations using deep learning. *Proceedings of the National Academy of Sciences*, 115(34):8505–8510, 2018.
- J. Han, J. Lu, and M. Zhou. Solving high-dimensional eigenvalue problems using deep neural networks: A diffusion Monte Carlo like approach. *Journal of Computational Physics*, 423:109792, 2020.
- G. Hardwick, S. Liang, and H. Yang. Solving high-dimensional partial integral differential equations: The finite expression method. *arXiv preprint arXiv:2410.00835*, 2024.
- K. Hornik, M. Stinchcombe, and H. White. Multilayer feedforward networks are universal approximators. *Neural networks*, 2(5):359–366, 1989.
- T. J. Hughes. *The finite element method: linear static and dynamic finite element analysis*. Courier Corporation, 2003.
- I. E. Lagaris, A. Likas, and D. I. Fotiadis. Artificial neural networks for solving ordinary and partial differential equations. *IEEE transactions on neural networks*, 9(5):987–1000, 1998.
- Y. LeCun, Y. Bengio, and G. Hinton. Deep learning. *nature*, 521(7553):436–444, 2015.
- R. J. LeVeque. *Finite difference methods for ordinary and partial differential equations: steady-state and time-dependent problems*. SIAM, 2007.
- M. Lewis, Y. Liu, N. Goyal, M. Ghazvininejad, A. Mohamed, O. Levy, V. Stoyanov, and L. Zettlemoyer. Bart: Denoising sequence-to-sequence pre-training for natural language generation, translation, and comprehension. *arXiv preprint arXiv:1910.13461*, 2019.
- Z. Li, N. Kovachki, K. Azizzadenesheli, B. Liu, K. Bhattacharya, A. Stuart, and A. Anandkumar. Fourier neural operator for parametric partial differential equations. *arXiv preprint arXiv:2010.08895*, 2020.
- S. Liang and H. Yang. Finite expression method for solving high-dimensional partial differential equations. *arXiv preprint arXiv:2206.10121*, 2022.
- L. Lu, P. Jin, and G. E. Karniadakis. Deeponet: Learning nonlinear operators for identifying differential equations based on the universal approximation theorem of operators. *arXiv preprint arXiv:1910.03193*, 2019.
- C. Raffel, N. Shazeer, A. Roberts, K. Lee, S. Narang, M. Matena, Y. Zhou, W. Li, and P. J. Liu. Exploring the limits of transfer learning with a unified text-to-text transformer. *Journal of machine learning research*, 21(140):1–67, 2020.
- M. Raissi, P. Perdikaris, and G. E. Karniadakis. Physics-informed neural networks: A deep learning framework for solving forward and inverse problems involving nonlinear partial differential equations. *Journal of Computational physics*, 378:686–707, 2019.
- C. Rudin. Stop explaining black box machine learning models for high stakes decisions and use interpretable models instead. *Nature machine intelligence*, 1(5):206–215, 2019.
- Z. Shen, H. Yang, and S. Zhang. Deep network with approximation error being reciprocal of width to power of square root of depth. *Neural Computation*, 33(4):1005–1036, 2021a.
- Z. Shen, H. Yang, and S. Zhang. Neural network approximation: Three hidden layers are enough. *Neural Networks*, 141:160–173, 2021b.
- J. Sirignano and K. Spiliopoulos. DGM: A deep learning algorithm for solving partial differential equations. *Journal of computational physics*, 375:1339–1364, 2018.

- Z. Song, M. K. Cameron, and H. Yang. A finite expression method for solving high-dimensional committor problems. *arXiv preprint arXiv:2306.12268*, 2023.
- Z. Song, C. Wang, and H. Yang. Finite expression method for learning dynamics on complex networks. *arXiv preprint arXiv:2401.03092*, 2024.
- R. Stevens, V. Taylor, J. Nichols, A. B. Maccabe, K. Yelick, and D. Brown. Ai for science: Report on the department of energy (doe) town halls on artificial intelligence (ai) for science. Technical report, Argonne National Lab.(ANL), Argonne, IL (United States), 2020.
- C. Szegedy. Intriguing properties of neural networks. *arXiv preprint arXiv:1312.6199*, 2013.
- E. F. Toro. *Riemann solvers and numerical methods for fluid dynamics: a practical introduction*. Springer Science & Business Media, 2013.
- B. Yu et al. The deep Ritz method: a deep learning-based numerical algorithm for solving variational problems. *Communications in Mathematics and Statistics*, 6(1):1–12, 2018.
- C. Zhang, S. Bengio, M. Hardt, B. Recht, and O. Vinyals. Understanding deep learning (still) requires rethinking generalization. *Communications of the ACM*, 64(3):107–115, 2021.
- S. Zhang, Z. Shen, and H. Yang. Deep network approximation: Achieving arbitrary accuracy with fixed number of neurons. *Journal of Machine Learning Research*, 23(276):1–60, 2022.
- Y. Zhu, N. Zabaras, P.-S. Koutsourelakis, and P. Perdikaris. Physics-constrained deep learning for high-dimensional surrogate modeling and uncertainty quantification without labeled data. *Journal of Computational Physics*, 394: 56–81, 2019.